

Selective area epitaxy of GaAs films using patterned graphene on Ge

Zheng Hui Lim,¹ Sebastian Manzo,¹ Patrick J. Strohbeen,¹
Vivek Saraswat,¹ Michael S. Arnold,¹ and Jason K. Kawasaki¹

¹*Materials Science and Engineering, University of Wisconsin-Madison, Madison, WI 53706*

(Dated: November 3, 2021)

We demonstrate selective area epitaxy of GaAs films using patterned graphene masks on a Ge (001) substrate. The GaAs selectively grows on exposed regions of the Ge substrate, for graphene spacings as large as 10 microns. The selectivity is highly dependent on the growth temperature and annealing time, which we explain in terms of temperature dependent sticking coefficients and surface diffusion. The high nucleation selectivity over several microns sets constraints on experimental realizations of remote epitaxy.

I. INTRODUCTION

Selective area epitaxy is a promising strategy for synthesis of confined quantum devices [1–3] and for reducing dislocation densities in highly lattice mismatched systems [4–7]. This growth mode is typically implemented by patterning openings in an inert dielectric mask such as SiO₂, on a crystalline substrate. The openings serve as selective nucleation sites for epitaxial film growth, while the mask defines the lateral dimensions and blocks dislocations from the substrate or film/substrate interface. Continued epitaxial lateral overgrowth can be used to produce coalesced planar films [4, 7–9].

Due to its chemical inertness, fast surface diffusion, and atomic thinness, patterned graphene is an attractive alternative mask material. Early studies demonstrated epitaxial lateral overgrowth of GaAs films on patterned multilayer graphite on a Si substrate, by liquid phase epitaxy (LPE) [10, 11]. More recently, monolayer graphene masks have been used to selectively nucleate GaN films at 75 nm openings on a SiC substrate [12], for GaN grown by metalorganic chemical vapor deposition (MOCVD). Open questions remain, however, about whether nucleation selectivity can be achieved using graphene over larger length scales, whether selectivity requires chemical precursors or can be achieved using physical vapor deposition techniques like molecular-beam epitaxy (MBE), and how growth kinetics affect the selectivity.

Here we demonstrate that monolayer graphene masks provide a highly selective barrier for selective area epitaxy of MBE-grown GaAs films, using patterned graphene stripes on a Ge (001) substrate. We demonstrate > 99% nucleation selectivity on the exposed Ge regions, for graphene stripe widths and spacings as large as 10 microns. The nucleation selectivity depends strongly on Ga surface diffusion and desorption, which we control experimentally by increasing the growth temperature and periodic anneal time. The high selectivity over a 10 micron scale also places constraints on experimental realizations of “remote epitaxy” [13], where the goal is to grow epitaxial films via remote interactions through continuous graphene with no intentional openings.

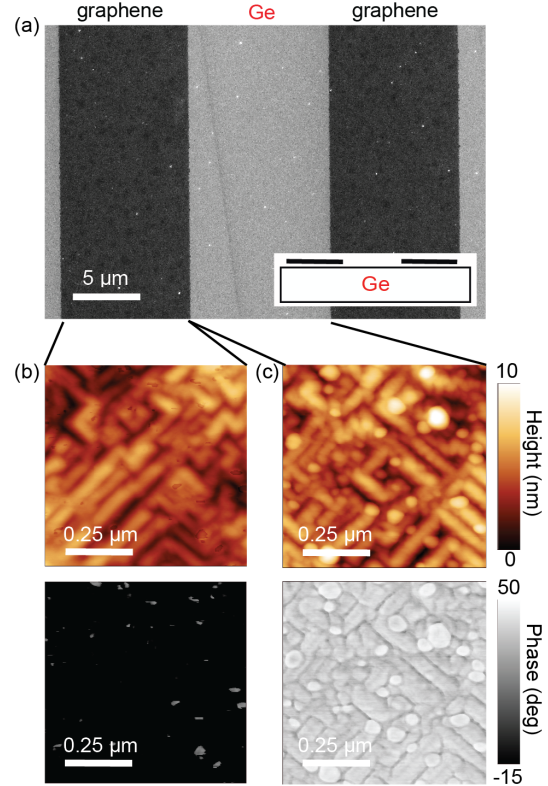


FIG. 1. **Patterned graphene on Ge (001).** (a) Scanning electron micrograph (SEM) image of the graphene mask with 10 μm feature size under in-lens secondary electron imaging mode. Inset shows the cartoon of graphene mask. (b) AFM height (top) and phase (bottom) images of a graphene region. (c) AFM images of an exposed Ge region.

II. RESULTS AND DISCUSSION

To make the patterned graphene on Ge, we first grow continuous monolayer graphene on a Ge (001) substrate by chemical vapor deposition using a methane precursor, following Refs. [14, 15]. We define the stripes by UV photolithography (Shipley 1813 photoresist), etch the exposed graphene regions using an oxygen plasma (50 W), and rinse the remaining photoresist using sequential acetone and isopropanol baths. The resulting patterned

template consists of alternating 5-10 microns wide stripes of graphene, separated by 5-10 microns of exposed Ge substrate (Fig. 1a). At this stage, scanning electron microscopy (SEM) confirms that the pattern is translated to the graphene with no obvious long-range tears (Fig. 1a).

Atomic force microscopy (AFM) images reveal a faceted morphology on both the graphene regions (Fig. 1b) and exposed Ge regions (Fig. 1c). The faceting is consistent with previous studies and is induced by graphene growth [16]. On the Ge regions we also observe spherical particles that we attribute to Ge that has been oxidized during the oxygen plasma etch. On graphene regions we observe ~ 10 nm diameter pinholes. These pinholes appear as bright spots in the AFM phase images, which we attribute to a different elastic modulus of graphene versus the Ge substrate. The pinholes are only faintly visible in the AFM height images. Based on these images we estimate a pinhole concentration of $\sim 40 \mu\text{m}^{-2}$, which is an order of magnitude smaller than the pinhole concentration for transferred graphene on GaAs (001) after native oxide desorption [17]. We attribute these pinholes to the photolithography and etching processes, since no pinholes were detected by AFM on the graphene/Ge samples before photolithography and etching.

Prior to GaAs film growth, we etch the exposed Ge oxides in a deionized water bath at 90°C . We then dry samples with nitrogen and immediately load them into a high vacuum loadlock ($p < 10^{-8}$ Torr) and outgas them at 150°C for at least 1 hour to remove organic residuals, followed by an anneal at 650°C in the ultrahigh vacuum MBE chamber ($p < 3 \times 10^{-10}$ Torr) to remove the remaining Ge-oxides. GaAs films are grown by MBE using elemental Ga from a standard effusion cell and a mixture of As_2/As_4 from a thermal cracker cell. Typical Ga fluxes were 2.74×10^{16} atoms/(cm^2s), calibrated by reflection high energy electron diffraction oscillations.

Fig. 2 shows scanning electron microscopy (SEM) and Raman spectroscopy for a GaAs film grown at 613°C by periodic supply of Ga and constant supply of As, on patterned graphene / Ge (001). We observe high nucleation selectivity for GaAs at exposed region of the Ge substrate, and negligible parasitic GaAs nucleation on the graphene mask. In the SEM image (Fig. 2a), the GaAs appears as coalesced islands with high secondary electron intensity on the Ge regions. We attribute the island morphology to the faceted Ge (001) surface, which is induced by graphene growth (Fig. 1c). Note that CVD graphene on (111) and (110)-oriented Ge is known to produce smoother surfaces [14], free from the faceting of the (001) surface. We expect that GaAs grown on these orientations may produce a smoother film surface morphology.

Raman spectroscopy maps (Horiba Labram, $\lambda = 532$ nm) of the GaAs TO and graphene 2D modes confirm that these islands are GaAs film, which grow preferentially on the exposed Ge (Fig. 2b) and not on the

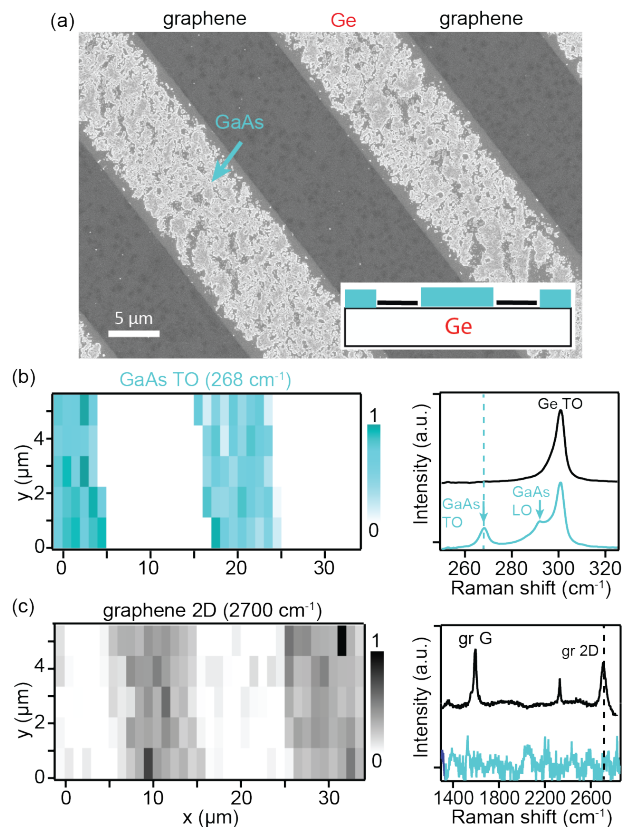


FIG. 2. **GaAs nucleation selectivity at the patterned openings.** (a) Secondary electron SEM image of a GaAs film nucleated on patterned graphene/Ge(001). The stripe pattern consists of 10 microns graphene and 10 microns of exposed Ge. (b) Left: Raman intensity map of the GaAs TO mode. Right: representative point spectra on a GaAs covered region and a graphene region. (c) Raman intensity map of the graphene 2D mode and corresponding spectra.

graphene mask (Fig. 2c). Representative point spectra on the GaAs-covered Ge regions (blue curves) and on the graphene regions (black curves) are shown on the right hand side of Figs 2(b) and (c). Note that in this scattering geometry, only the GaAs LO mode is symmetry allowed for a perfect GaAs crystal – the GaAs TO mode is not symmetry allowed [18]. We attribute the presence of a GaAs TO mode to strain or point defects.

We find that the selectivity for GaAs growth on Ge rather than the graphene mask is highly dependent on the growth temperature and annealing. Figure 3(a) shows SEM images of GaAs films grown by codeposition of Ga and As, at varying substrate temperature. All samples were exposed to a total flux of 4.56×10^{14} Ga atoms/ cm^2 , which would correspond to a GaAs film thickness of 14 nm for a Ga sticking coefficient of 1. In these images the GaAs corresponds to the light islands, the graphene corresponds to the dark stripes, and the Ge corresponds to lighter stripes. At a growth temperature of 580°C , the concentration of parasitic nucleated islands on graphene is $\sim 10 \mu\text{m}^{-2}$, which is slightly less than the $\sim 40 \mu\text{m}^{-2}$

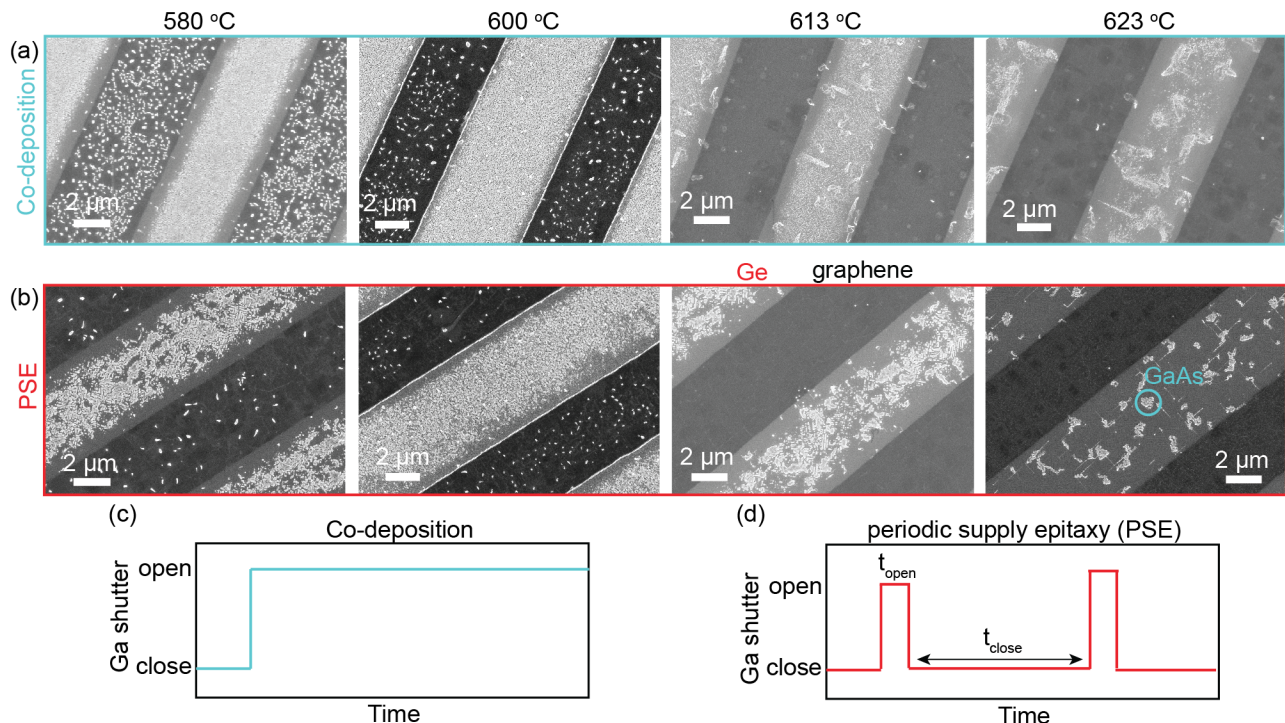


FIG. 3. **Enhancing selectivity with growth temperature and periodic supply epitaxy (PSE).** (a) SEM images of GaAs grown by co-deposition, for increasing growth temperature. (b) SEM images for samples grown by PSE. (c) Schematic of co-deposition. The Ga shutter is kept open for the entire growth. (d) Schematic of PSE. The Ga shutter is periodically shuttered open and closed.

concentration of graphene pinholes before GaAs growth (Fig. 1b). We hypothesize that the parasitic GaAs growth on graphene is caused by nucleation in the pinholes. Similar nucleation at pinholes is observed for GaAs films grown on unpatterned graphene/GaAs (001) [17]. Further optimization is required to reduce the graphene pinhole density created during lithography and etching.

With increasing growth temperature, the amount of GaAs nucleated on both graphene and Ge regions decreases, i.e. the sticking coefficient decreases. The rate of GaAs sticking on graphene decreases more rapidly than on Ge, such that for a growth temperature of 613 °C there is negligible GaAs growth on graphene and highly preferred growth on Ge. We quantify these effects in Fig. 4. Here, A_{Ge}^{codep} is the area fraction of GaAs on the exposed Ge regions and A_{gr}^{codep} is the area fraction of GaAs on graphene (Supplemental Information). We define the selectivity as $S = A_{Ge}/(A_{gr} + A_{Ge})$. At growth temperatures greater than 610 °C we obtain a selectivity $S > 99\%$.

We further enhance the nucleation selectivity by employing periodic supply epitaxy (PSE). Here, we fix the As shutter open and periodically modulate the Ga shutter between the open position (GaAs growth) and the closed position (annealing, Fig. 3d). Fig. 3b shows SEM images of GaAs films grown by PSE, where we let $t_{growth} = 1$ minute and $t_{close} = 6$ minutes, for a total of 15 cycles. We find that PSE decreases the total stick-

ing coefficient (Fig. 4a) and increases the selectivity for GaAs nucleation on Ge compared to on graphene (Fig. 4b).

We understand effects of temperature and anneal time in terms of the microscopic processes sketched in Fig. 4b insert. High selectivity results from a combination of fast surface diffusion on graphene and high desorption rate from graphene, compared to Ge which has a sticking coefficient closer to 1. Upon arrival at the surface, Ga adatoms diffuse over a characteristic length λ . Ga adatoms will then either desorb into the vapor or attach to the surface to form GaAs. With increasing temperature, the desorption rate of Ga from graphene decreases dramatically, as observed by the factor of 10^3 drop in GaAs surface coverage on graphene (A_{gr}) from 560 to 625 °C (Fig. 4a). In contrast, for the same range of temperatures the GaAs coverage on Ge (A_{Ge}) decreases by less than a factor of 10. Surface diffusion also increases with temperature, resulting in an increased probability for Ga to diffuse and attach to reactive areas of the exposed Ge substrate. These combined factors explain the general observation that increasing the temperature increases the selective growth on Ge. Increasing the anneal time by periodic supply epitaxy plays a similar role as temperature, by increasing the time for desorption and increasing the diffusion length λ . These general trends are consistent with selective area growth using conven-

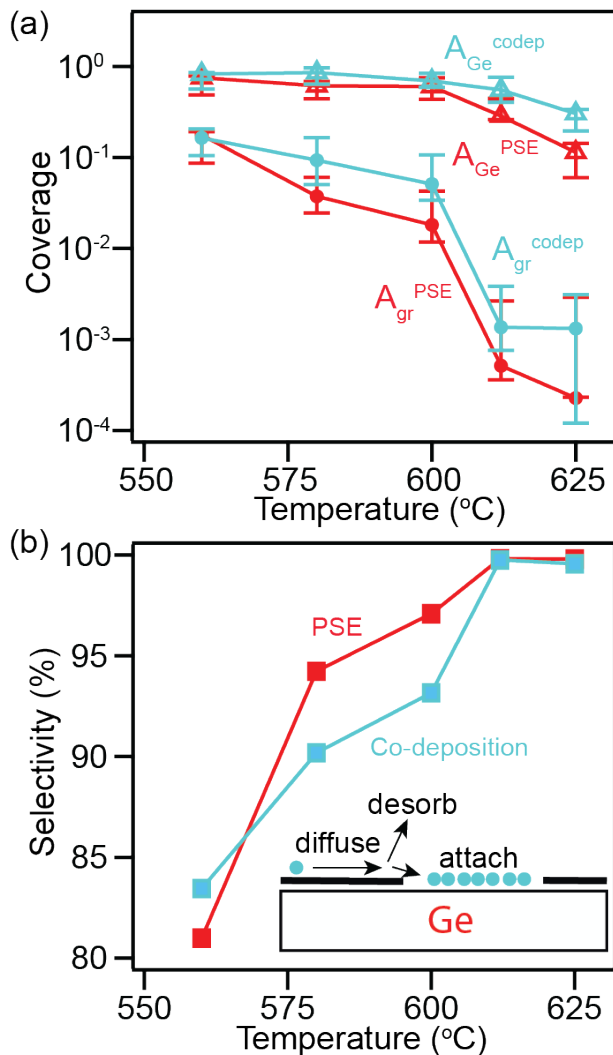


FIG. 4. **Quantification of selectivity.** (a) Percent area coverage of GaAs film nucleated on exposed Ge regions (A_{Ge}) and on graphene regions (A_{gr}), for growth by co-deposition and by periodic supply epitaxy. The percent area coverage was determined from the SEM images. (b) Nucleation selectivity $S = A_{\text{Ge}} / (A_{\text{Ge}} + A_{\text{gr}})$ on the exposed Ge regions.

tional SiO_2 masks [8].

The high selectivity and long diffusion length also set constraints for experimental realizations of “remote epitaxy” on unpatterned graphene. “Remote epitaxy” refers to the epitaxial growth of a film on a continuous graphene-terminated substrate, with no intentional openings. In this growth mode, epitaxial registry between film and substrate is thought to occur via “remote” interac-

tions that permeate through graphene. However, pinholes or openings in the graphene can serve as alternate nucleation sites, followed by lateral overgrowth [17] or growth by intercalation [19]. In the present work, our results show that GaAs can nucleate at graphene openings over length scales as large as 10 microns. Experimental realizations of remote epitaxy may require graphene defect control over a length scale of several microns, in order to clearly distinguish a “remote” mechanism from a selective area and lateral epitaxy mechanism.

III. CONCLUSIONS

We demonstrated selective area epitaxy of GaAs using a patterned graphene mask on Ge (001), over a length scale of 10 microns. The selectivity is comparable to previous demonstrations of selective area epitaxy by MBE using SiO_2 masks, where smaller spacings of a 100 nm to 2 microns are more typical [9, 20, 21]. The main limiting feature in the current work is the rough surface morphology of GaAs on Ge (001), which we attribute to graphene-induced faceting of the Ge (001) surface. We expect that growth on graphene/Ge in (111) or (110) orientation may be a path for smoother films, since these orientations do not produce the large graphene-induced faceting. Further improvements in lithography and etching may also be required to reduce the graphene pinholes and enhance the selectivity for growth at temperatures below 600°C.

IV. ACKNOWLEDGMENTS

This work was primarily supported by the Defense Advanced Research Projects Administration (DARPA Grant number D19AP00088). Graphene synthesis and characterization are supported by the U.S. Department of Energy, Office of Science, Basic Energy Sciences, under award no. DE-SC0016007. GaAs film characterization was supported by the NSF Division of Materials Research through the University of Wisconsin Materials Research Science and Engineering Center (Grant No. DMR-1720415) and the CAREER program (DMR-1752797). We gratefully acknowledge the use of Raman and electron microscopy facilities supported by the NSF through the University of Wisconsin Materials Research Science and Engineering Center under Grant No. DMR-1720415.

[1] Q. Gao, D. Saxena, F. Wang, L. Fu, S. Mokkalapati, Y. Guo, L. Li, J. Wong-Leung, P. Caroff, H. H. Tan, et al., *Nano letters* **14**, 5206 (2014).

[2] P. Aseev, A. Fursina, F. Boekhout, F. Krizek, J. E. Sestofo, F. Borsoi, S. Heedt, G. Wang, L. Binci, S. Martí-Sánchez, et al., *Nano letters* **19**, 218 (2018).

- [3] J. S. Lee, S. Choi, M. Pendharkar, D. J. Pennachio, B. Markman, M. Seas, S. Koelling, M. A. Verheijen, L. Casparis, K. D. Petersson, et al., *Physical Review Materials* **3**, 084606 (2019).
- [4] Y. Ujiie and T. Nishinaga, *Japanese Journal of Applied Physics* **28**, L337 (1989).
- [5] E. Fitzgerald and N. Chand, *Journal of electronic materials* **20**, 839 (1991).
- [6] J.-S. Park, J. Bai, M. Curtin, B. Adekore, M. Carroll, and A. Lochtefeld, *Applied Physics Letters* **90**, 052113 (2007).
- [7] W. E. McMahon, M. Vaisman, J. D. Zimmerman, A. C. Tamboli, and E. L. Warren, *APL Materials* **6**, 120903 (2018).
- [8] T. Nishinaga, T. Nakano, and S. Zhang, *Japanese journal of applied physics* **27**, L964 (1988).
- [9] D. J. Ironside, A. M. Skipper, T. A. Leonard, M. Radulaski, T. Sarmiento, P. Dhingra, M. L. Lee, J. Vuckovic, and S. R. Bank, *Crystal Growth & Design* **19**, 3085 (2019).
- [10] Z. Zytkeiwicz, J. Domagała, and D. Dobosz, *Journal of Applied Physics* **90**, 6140 (2001).
- [11] Z. Zytkeiwicz, J. Domagała, D. Dobosz, and J. Bak-Misiuk, *Journal of applied physics* **84**, 6937 (1998).
- [12] R. Puybaret, G. Patriarche, M. B. Jordan, S. Sundaram, Y. El Gmili, J.-P. Salvestrini, P. L. Voss, W. A. De Heer, C. Berger, and A. Ougazzaden, *Applied Physics Letters* **108**, 103105 (2016).
- [13] Y. Kim, S. S. Cruz, K. Lee, B. O. Alawode, C. Choi, Y. Song, J. M. Johnson, C. Heidelberger, W. Kong, S. Choi, et al., *Nature* **544**, 340 (2017).
- [14] B. Kiraly, R. M. Jacobberger, A. J. Mannix, G. P. Campbell, M. J. Bedzyk, M. S. Arnold, M. C. Hersam, and N. P. Guisinger, *Nano Lett.* **15**, 7414 (2015).
- [15] G. Wang, M. Zhang, Y. Zhu, G. Ding, D. Jiang, G. Qinglei, S. Liu, X. Xie, P. K. Chu, Z. Di, et al., *Sci. Rep.* **3**, 2465 (2013).
- [16] K. M. McElhinny, R. M. Jacobberger, A. J. Zaugg, M. S. Arnold, and P. G. Evans, *Surface Science* **647**, 90 (2016).
- [17] S. Manzo, P. J. Strohbeen, Z.-H. Lim, V. Saraswat, M. S. Arnold, and J. K. Kawasaki, arXiv preprint arXiv:2106.00721 (2021).
- [18] G. Abstreiter, E. Bauser, A. Fischer, and K. Ploog, *Applied physics* **16**, 345 (1978).
- [19] N. Briggs, B. Bersch, Y. Wang, J. Jiang, R. J. Koch, N. Nayir, K. Wang, M. Kolmer, W. Ko, A. D. L. F. Duran, et al., *Nature materials* **19**, 637 (2020).
- [20] S. Lee, K. Malloy, L. Dawson, and S. Brueck, *Journal of applied physics* **92**, 6567 (2002).
- [21] G. Bacchin and T. Nishinaga, *Journal of crystal growth* **211**, 389 (2000).

V. SUPPORTING INFORMATION

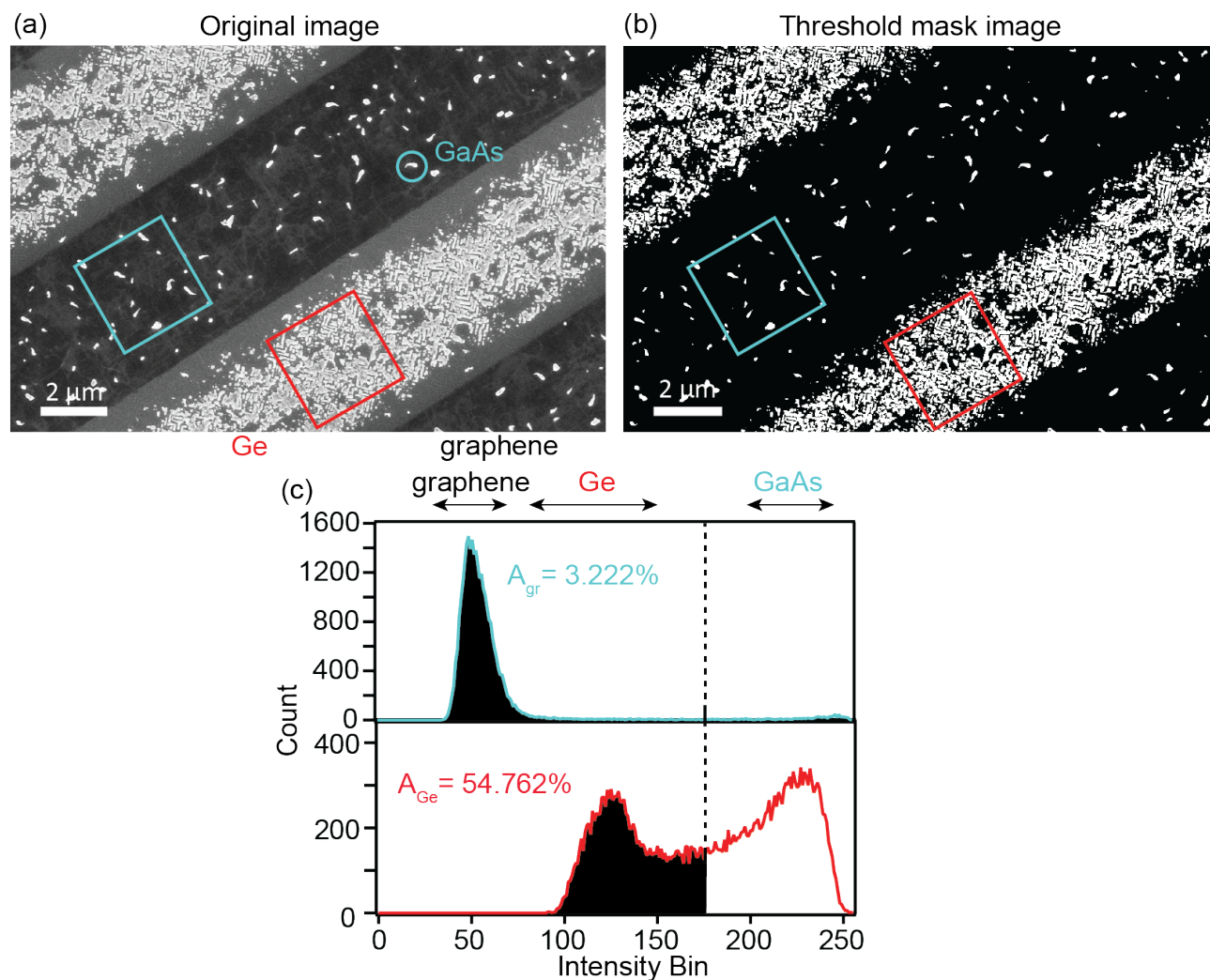


FIG. S-1. **Determination of surface coverage.** (a) SEM image of a GaAs film grown at 580°C. (b) Threshold mask image, used to determine the areal coverage of GaAs film. (c) Histograms of the pixel intensity for the red and blue boxed regions. Distinct peaks in the histograms correspond to Ge, graphene, and GaAs. The threshold for the mask is shown as the dashed line: pixels with intensity higher than this threshold correspond to GaAs. The threshold is determined based on the mid-point between the FWHM of graphene and GaAs peaks.